Cusp observations of high- and low-latitude reconnection for northward IMF

S. A. Fuselier, K. J. Trattner, and S. M. Petrinec
Lockheed Martin Advanced Technology Center, Palo Alto, California

C. T. Russell and G. Le
Institute of Geophysics and Planetary Physics, University of California, Los Angeles, California

Abstract. POLAR/Toroidal Imaging Mass Angle Spectrograph (TIMAS) observations in the cusp reveal evidence of both high- and low-latitude reconnection during high solar wind dynamic pressure, northward IMF intervals. Under these restrictive conditions, the magnetic field observed by the POLAR/Magnetic Fields Investigation in the northern cusp often rotates from lobe-like orientations (B_z<0, B_x>0) to dayside magnetospheric-like orientations (B_z >0, B_x <0). Proton distributions observed when the magnetic field has a magnetospheric-like orientation are consistent with either reconnection poleward of the cusp at high latitudes or reconnection equatorward of the cusp at lower latitudes. Transitions from one type of proton distribution to another as the field rotates from lobe-like to dayside magnetospheric-like orientations indicate sunward (poleward) convection of the reconnected magnetic field for reconnection poleward (equatorward) of the cusp. A survey of 17 intervals of high solar wind dynamic pressure and northward IMF indicates that these two reconnection topologies occur with approximately equal probability and that reconnection equatorward of the cusp favors small angles between the magnetosheath and dayside magnetospheric magnetic fields.

1. Introduction

The interconnection of magnetic fields through magnetic reconnection is an important if not dominant process for mass, energy, and momentum transfer from the Earth's magnetosheath to the magnetosphere. While reconnection is generally recognized as important, the details of the process remain poorly understood. One of the least understood details is why certain magnetic field configurations and initial conditions lead to the initiation of reconnection.

If reconnection is assumed to occur between magnetic fields of exactly opposite polarity, then magnetosheath and magnetospheric field lines should reconnect near the subsolar magnetopause when the Interplanetary Magnetic Field (IMF) is southward [*Dungey*, 1961]. This type of reconnection is referred to as anti-parallel reconnection. The reconnected field lines convect poleward and tailward away from the subsolar region. There is ample evidence that reconnection at the dayside magnetopause occurs for southward IMF conditions although observations indicate that purely anti-parallel fields are not a necessary condition for this process [e.g., *Gosling et al.*, 1990]. In fact, shear angles as small as 50˚ were observed between the magnetosheath and magnetospheric magnetic fields participating in reconnection. Reconnection between magnetic fields that are not strictly anti-parallel is referred to as component reconnection.

When the IMF is northward, anti-parallel reconnection between magnetosheath and magnetospheric magnetic fields must occur at high latitudes poleward of the Earth's magnetic cusps [*Dungey*, 1963]. These reconnected field lines would convect first sunward and then eventually tailward away from the high latitude reconnection site. There is ample evidence that this reconnection occurs between magnetosheath magnetic field lines draped against the magnetopause and high latitude magnetospheric field lines in the lobe. At the high latitude magnetopause, this evidence consists of so-called "D" shaped ion distributions (i.e., distributions with a low speed cutoff parallel or anti-parallel to the magnetic field) in the magnetospheric boundary layer [e.g., *Gosling et al.*, 1991; *Kessel et al.*, 1996]. These "D" distributions are not unique to northward IMF conditions, were predicted prior to their discovery, and are the result of acceleration of

magnetosheath ions across the open magnetopause [e.g., *Cowley,* 1982]. For these few cases at the high latitude magnetopause, the shear angle between the magnetospheric and magnetosheath field lines was very nearly 180˚, consistent with antiparallel reconnection.

For any finite dawn/dusk (B_y) component to the interplanetary magnetic field, magnetosheath magnetic field lines draped against the magnetopause will reconnect poleward of only one of the magnetic cusps [e.g., *Russell,* 1972]. As the reconnected, draped magnetic field line is incorporated into the magnetosphere, the effects of high-latitude reconnection are observable at lower latitudes down to the equatorial magnetopause. Energetic electrons streaming in a layer just sunward of the subsolar magnetopause is an example of these effects [*Fuselier et al.,* 1995; 1997].

Evidence of high latitude reconnection and sunward convection of reconnected field lines is also found in the Earth's magnetospheric cusps. Ground magnetograms and auroral emissions show evidence of sunward convection over the polar cap [e.g., *Maezawa,* 1976; *Øieroset et al.,* 1997]. Direct evidence of sunward convection of the entering magnetosheath plasma is seen in low and mid-altitude spacecraft observations in the cusp [e.g., *Woch and Lundin,* 1992]. This evidence consists of so-called "reverse" ion dispersion whereby the observed energy of the precipitating magnetosheath ion distribution decreases with decreasing the invariant latitude. (In "normal" ion dispersion observed for southward IMF conditions, the energy decreases with increasing invariant latitude [e.g., *Onsager et al.,* 1993].) The reverse ion dispersion is a direct result of the time-of-flight or velocity filter effect produced by the reconnection and subsequent sunward convection of the reconnected field line. From mid-altitudes to the magnetopause, the magnetosheath population propagating toward the ionosphere and a return population that mirrored at low latitudes can be observed [e.g., *Gosling et al.,* 1991; *Woch and Lundin,* 1992].

While there is ample evidence for high-latitude, anti-parallel reconnection poleward of the cusp for northward IMF, there is also evidence that reconnection can occur at lower latitudes equatorward of the cusp for northward IMF. This is necessarily component reconnection since the magnetosheath and magnetospheric field lines are not anti-parallel equatorward of the cusp [e.g.,

Crooker, 1979]. In fact, angles between the magnetospheric and magnetosheath magnetic fields can be very small and it is often argued that this prevents reconnection from occurring equatorward of the cusp [see however, *Anderson et al.*, 1997].

Ion and electron distributions near the subsolar magnetopause consistent with reconnection equatorward of the cusp were observed during intervals of high solar wind dynamic pressure [*Onsager and Fuselier*, 1994; *Fuselier et al.*, 1997]. Some auroral emissions in the cusp for northward IMF conditions are also consistent with reconnection equatorward of the cusp [e.g., *Øieroset et al.*, 1997; *Sandholt et al.*, 1998]. Finally, recent observations from the Polar spacecraft in the high-altitude cusp are also consistent with reconnection equatorward of the cusp [*Chandler et al.*, 1999]. Like the observations near the subsolar magnetopause, these recent cusp observations were obtained under high solar wind dynamic pressure conditions.

In this paper, the large data set of recent Polar observations is exploited to investigate the occurrence of both high-latitude (poleward of the cusp) anti-parallel reconnection and low-latitude (equatorward of the cusp) component reconnection under northward IMF, high solar wind dynamic pressure conditions.

Observations in this paper are from the Polar spacecraft in the cusp and the Wind spacecraft in the solar wind. The Polar spacecraft was launched into a nearly 90˚ inclination orbit with an apogee of 9 R_E. The orbit precesses in local time so that twice a year for a few months it cuts through the dayside northern cusp region at high altitudes. The Wind spacecraft provides simultaneous context measurements in the solar wind for a range of distances from near the bow shock to near L1 (15 to ~240 R_E upstream from the Earth). Timing of these observations was corrected for propagation of the plasma from the Wind spacecraft to the bow shock, through the magnetosheath, and into the cusp.

Proton observations in this paper are from the Polar/Toroidal Imaging Mass-Angle Spectrograph (TIMAS) [*Shelley et al.*, 1995]. This energetic ion mass spectrometer measures full 3-dimensional distributions (14 energies by 14 polar angles by 16 azimuth angles) for several ion species in one spacecraft spin (6 s). In this paper, only the proton distributions are presented.

Magnetic field measurements are from the Polar/Magnetic Fields Investigation [*Russell et al.*, 1995]. This magnetometer makes a vector magnetic field measurement at a standard rate of ~0.1 s. In this paper, data are spin averaged to determine proton pitch angle distributions and averaged over 1 minute to determine cusp magnetic field magnitudes and orientations.

Two instruments on the Wind spacecraft provide context measurements for the cusp observations. Solar wind plasma bulk flow speeds and densities are obtained from the Wind/Solar Wind Experiment [*Ogilvie et al.*, 1995]. The solar wind magnetic field is obtained from the Wind/Magnetic Field Investigation [*Lepping et al.*, 1995]. All solar wind context measurements in this paper were obtained from the NASA CDAWeb.

The outline of this paper is as follows: In Section 2, cusp observations on 20 June 1996 consistent with anti-parallel reconnection poleward of the cusp are presented. In Section 3, cusp observations on 11 April 1997 consistent with component reconnection equatorward of the cusp are presented. In Section 4, a survey of 17 cusp events is presented. In Section 5, the events in Sections 2 and 3 and the survey in Section 4 are discussed.

2. 20 June 1996 Cusp Event

Figure 1 shows an overview of the 20 June 1996 cusp event. At the top is a noon-midnight meridian cut through the magnetosphere showing the Polar spacecraft trajectory from 0300 to 0800 UT. During this interval, the spacecraft was nearly in this plane. The magnetosphere is shown in an uncompressed state; however, the solar wind magnetic field was strongly northward and the solar wind dynamic pressure was ~4 times the nominal solar wind dynamic pressure during the event. Therefore, the magnetosphere was probably compressed so that its subsolar standoff distance was ~8 R_E from the Earth [e.g., *Petrinec and Russell*, 1996].

Below the schematic magnetosphere in Figure 1 are the three components and the magnitude of the magnetic field in the cusp region for the period from 0300 to 0800 UT. The solid lines show the observed magnetic field and the dashed lines shows the Tsyganenko 1996 model

magnetic field. During the interval, the model predicts that the spacecraft slowly transitions from magnetic field lines with $B_{xGSM} < 0$ to field lines with $B_{xGSM} > 0$. Because the apogee of the spacecraft is only 9 R_E and the uncompressed magnetopause at high latitudes is at a radial distance of ~12 R_E, the magnetic field model predicts that the spacecraft remained on magnetic field lines with $B_z<0$ throughout the interval from 0300 to 0800 UT. The model magnetic field lines throughout the interval are consistent with those found in the lobe (located poleward of the cusp). These lobe-like field lines ultimately form part of the Earth's magnetotail.

Prior to 0450 UT and after 0700 UT, the observed and model field agree reasonably well. However, most of the time between 0500 and 0700 UT, the observed and model magnetic field had nearly opposite orientation. In particular, there are long periods with $B_x<0$ and $B_z>0$ when the model magnetic field predicts the opposite polarity. The total magnetic field was also considerably weaker than that predicted by the model. In the dayside magnetosphere, magnetic field lines with $B_x<0$ and $B_z>0$ are found equatorward of the cusp. These "dayside magnetospheric-like" field lines ultimately form part of the dayside outer magnetosphere (i.e. they map to the dayside equatorial region) and are topologically distinct from lobe-like magnetic field lines poleward of the cusp that map to the tail.

The Polar spacecraft observes these magnetospheric-like magnetic field lines only because the high solar wind dynamic pressure compresses the magnetopause. This compression moves the effective position of the spacecraft from a location poleward of the cusp and relatively far from the magnetopause to a location equatorward of the cusp and relatively near the magnetopause. If the solar wind dynamic pressure is large enough, then the magnetopause can move in far enough for the spacecraft to exit the magnetosphere and enter the magnetosheath. Since the solar wind magnetic field was strongly northward during the interval in Figure 1, the $B_x<0$ and $B_z>0$ magnetic field orientation between 0500 and 0700 UT is also consistent with the orientation of the magnetosheath magnetic field that is draped against the high latitude magnetopause. However, the model magnetopause location for the observed solar wind dynamic pressure [e.g., *Petrinec and*

Russell, 1996] suggests that the spacecraft remained in the magnetosphere. Furthermore, the ion distributions discussed below are inconsistent with those found in the high latitude magnetosheath.

During the interval of depressed magnetic field strength from 0500 to 0700 UT in Figure 1, significant fluxes of magnetosheath protons were observed, consistent with the spacecraft location in the cusp. Figure 2 shows two proton distributions observed during this cusp interval. Shown are two dimensional cuts through the three dimensional distributions measured by the TIMAS instrument. The distributions are in the spacecraft frame of reference and the plane of the cut contains the magnetic field direction (along the y-axis) and the Earth-sun direction. There are two contours per decade of phase space density and the dots show the centers of the energy/angle bins used to produce the contours. Angle bin centers within $\pm 20^{\circ}$ of the plane of the cut were rotated into the plane (i.e., preserving total energy) to produce the distributions in Figure 2. Below each two dimensional distribution is a slice through the distribution along the magnetic field. In these one dimensional slices, positive velocities are parallel to the magnetic field, solid lines show the measured phase space density, and dashed lines show the 1σ level.

The distribution on the left-hand side was obtained when the magnetic field had a lobe-like orientation (see the interval marked L in Figure 1). The distribution on the right-hand side was obtained when the magnetic field had a dayside magnetospheric-like orientation (see the interval marked M in Figure 1). The distribution on the left-hand side consists of two distinct populations. The first is a relatively high flux, low energy, parallel propagating proton population that has a low energy cutoff parallel to the magnetic field. The second is a higher energy, lower flux, anti-parallel propagating proton population that has a low energy cutoff anti-parallel to the magnetic field. The distribution on the right-hand side resembles a near-isotropic, single population with a small bulk flow parallel to the magnetic field.

Distributions consisting of two distinct populations with low speed cutoffs have been observed previously in the high latitude magnetosphere [e.g., *Gosling et al.*, 1991; *Woch and Lundin*, 1992]. Previously, these distributions were interpreted in terms of magnetic reconnection and the velocity filter effect caused by the convection of the reconnected field line. The

distributions in Figure 2 are interpreted in the same way as in these previous studies. Under this interpretation, the two proton populations in the left-hand panel of Figure 2 provide both qualitative and quantitative information on the topology of the magnetic field line and the location of the reconnection site. The higher energy, lower flux, anti-parallel propagating proton distribution consists of magnetosheath ions that have propagated along the reconnected magnetic field to the ionosphere, reflected, and returned to the spacecraft. Therefore, the direction of propagation of this population indicates that the spacecraft was on a magnetic field line that had a low altitude mirror point or a "foot" in the northern ionosphere. This is not surprising considering the location of the spacecraft in the high latitude northern magnetosphere (see Figure 1). The lower energy, higher flux, parallel propagating population in Figure 2 came directly from the reconnection site. Therefore, the reconnection site was located opposite the direction of propagation of this population or in the direction anti-parallel to the magnetic field. Since the magnetic field orientation was lobe-like ($B_x>0$, $B_z<0$), the direction of motion of this population and the model field in Figure 1 indicate that the reconnection site was poleward of the cusp at high latitudes.

One important consequence of the velocity filter effect is that protons near the low speed cutoffs of the parallel and anti-parallel propagating populations originated very near the reconnection site. Since these protons arrive at the same time at the spacecraft, the population that propagated along the magnetic field from the reconnection site to the ionosphere and returned from the low altitude mirror point must have a higher velocity than the population that arrived directly from the reconnection site. Using the equivalent arrival times of the ions at the two low speed cutoffs, the ratio of the distance from the spacecraft to the reconnection site (X_r) to the distance from the spacecraft to the low altitude mirror point (X_m) is given by [Onsager et al., 1990]:

$$X_r / X_m = 2 V_e / (V_m - V_e) \quad (1)$$

Here, V_e is the low speed cutoff of the parallel propagating population (toward the Earth) and V_m is the low speed cutoff of the anti-parallel propagating population (from the low altitude mirror

point). In the distribution on the left-hand side of Figure 2, the low speed cutoff of the parallel propagating population is not as distinct as the cutoff of the antiparallel propagating population. However, estimating $V_e = 50 \pm 25$ km/s, $V_m = 300 \pm 10$ km/s, $X_m = 8\ R_E$ (see Figure 1), and using (1), the distance from the spacecraft to the reconnection site is estimated to be $X_r = 3.3 \pm 2\ R_E$. The uncertainty in X_r arises primarily from the difficulty in estimating V_e (and its error). It is concluded that the spacecraft was between 1 and 5 R_E from the reconnection site that is located poleward of the cusp.

For reconnection poleward of the cusp, the reconnected magnetic field lines convect sunward as they are incorporated into the magnetosphere. Reconnected field lines and the magnetosheath distributions on these field lines evolve during this convection. On these evolved field lines, magnetosheath protons propagating parallel to the magnetic field enter equatorward of the spacecraft location and protons propagating antiparallel to the magnetic field have reflected from the low altitude mirror point (see the schematic at the top of Figure 1). The "low energy cutoffs" of both distributions are at very low energies and the distribution appears nearly isotropic, as in the right-hand panel of Figure 2. No estimate of the distance to the reconnection site is possible since the low energy cutoffs cannot be measured.

Although the field line orientation for the right-hand distribution in Figure 2 was consistent with that in the magnetosheath, the distribution itself is not consistent with a proton distribution in the magnetosheath at high latitudes. At these high latitudes near the magnetopause, the proton distribution should have a velocity that is a significant fraction (~0.5 to 0.75) of the solar wind velocity [e.g., Onsager et al., 1995]. Since the solar wind bulk flow velocity during this interval was 460 km/s, the magnetosheath distribution should have a velocity of >230 km/s. In contrast, distribution in the right-hand panel of Figure 2 has a bulk flow velocity of ~50 km/s parallel to the magnetic field. Thus, it is concluded that the spacecraft remained in the magnetosphere during the interval in Figure 1.

The distributions in Figure 2 are representative of the lobe-like and dayside magnetospheric-like intervals throughout the period from 0500 to 0600 UT. At 6 second

resolution, this time period contains 600 lobe-like and magnetospheric-like distributions. After 0600 UT, the TIMAS instrument switched to a different mode and distributions such as those in Figure 2 could no longer be produced.

3. 11 April 1997 Cusp Interval

Figure 3 shows an overview of the 11 April 1997 cusp event. The format of this figure is identical to that of Figure 1. The solar wind magnetic field was strongly northward during this interval and the solar wind dynamic pressure was ~6 times the nominal solar wind dynamic pressure. Therefore, the magnetosphere was probably compressed so that the subsolar magnetopause distance was <8 R_E from the Earth.

During the interval from 1100 to 1600 UT in Figure 3, the model predicts that the spacecraft slowly transitions from magnetic field lines with $B_{xGSM}<0$ to field lines with $B_{xGSM}>0$. Because the apogee of the Polar orbit is only 9 R_E and the uncompressed magnetopause at high latitudes is at a radial distance of ~12 R_E, the magnetic field model predicts that the spacecraft should remain on lobe-like magnetic field lines (with $B_z<0$) throughout the interval from 1100 to 1600 UT.

For most of the interval, the observed and model magnetic field in Figure 3 agree quite well. However, from 1430 to 1450 UT, $B_x<0$ and $B_z>0$ when the model predicts the opposite polarity. There are also significant dips in the observed total magnetic field during these times. This dayside magnetospheric-like magnetic field interval in Figure 3 is similar in many respects to the much longer interval in Figure 1.

As in the event in Figure 1, the Polar spacecraft observes magnetic fields with dayside magnetospheric-like orientation in Figure 3 only because the high solar wind dynamic pressure compresses the magnetopause. This compression moves the effective position of the spacecraft from lobe-like magnetic field lines poleward of the cusp and relatively far from the magnetopause to magnetospheric-like magnetic field lines equatorward of the cusp and relatively near the

magnetopause. As in the interval in Figure 1, the magnetospheric-like magnetic field orientation in Figure 3 is also consistent with the magnetic field orientation in the high latitude magnetosheath. However, as in the event in Figure 1, the solar wind dynamic pressure during the event in Figure 3 was not sufficient to move the magnetopause earthward of the spacecraft and the ion distributions discussed below are inconsistent with those found in the magnetosheath at high latitudes.

During the interval from 1430 to 1450 UT, significant fluxes of magnetospheric protons were observed, consistent with the spacecraft location in the cusp. Figure 4 shows two proton distributions observed during this cusp interval in Figure 3. The format is identical to that in Figure 2. The distribution on the left-hand side was obtained when the magnetic field had a lobe-like orientation (see the interval marked L in Figure 3). The distribution on the right-hand side was obtained when the magnetic field had a dayside magnetospheric-like orientation (see the interval marked M in Figure 1). Comparing the distributions in Figures 2 and 4, it is clear that the type of distribution observed for lobe-like magnetic field orientations on 20 June 1996 was observed for dayside magnetospheric-like orientations on 11 April 1997. Similarly, the type of distribution observed for dayside magnetospheric-like magnetic field orientations on 20 June 1996 was observed for lobe-like orientations on 11 April 1997.

Using the same interpretation as in the previous section, the two proton populations that make up the distribution on right-hand side of Figure 4 provide qualitative and quantitative information on the location of the spacecraft relative to the reconnection site. On the right-hand side of Figure 4, the anti-parallel propagation of the higher energy, lower flux, population indicates that the spacecraft was on a magnetic field line that had one foot in the northern ionosphere. The parallel propagation of the lower energy, higher flux population indicates that the reconnection site was located in the anti-parallel direction from the spacecraft. Because this population is observed on a field line with dayside magnetic field orientation, this propagation direction places the reconnection site equatorward of the spacecraft at “low” latitudes equatorward of the cusp. This parallel propagating distribution observed during the magnetospheric-like interval and the

implications of these observations for another Polar event are discussed in detail in Chandler et al. [1999].

As in the previous section, estimates of the low speed cutoffs of the parallel and anti-parallel propagating populations in Figure 4, the distance to the low altitude mirror point, and (1) yields the distance from the spacecraft to the reconnection site. The parallel and anti-parallel propagating populations in the right-hand side of Figure 4 have very indistinct low speed cutoffs. In fact, one interpretation is that the low speed cutoff of the parallel propagating distribution is less than zero. A low speed cutoff that is less than zero would invalidate the use of (1) and would require a different interpretation of the two ion populations than the interpretation presented here. Possible explanations for an indistinct low speed cutoff in the parallel direction include ionospheric outflow at low energies and wave-particle scattering. Both of these possibilities result in proton populations propagating antiparallel to the magnetic field at very low energies, thus rendering indistinct the low speed cutoff of the parallel propagating population. Finally, the TIMAS instrument suffers from a saturation effect which can elevate the countrate in angle bins with low counts if the countrate is very high in another angle bin that is measured simultaneously.

Assuming that the low speed cutoff of the parallel propagating population in the right-hand side of Figure 4 is small but greater than zero, estimating V_e = 25±10 km/s, V_m = 450±50 km/s, X_r = 8 R_E (see Figure 3), and using (1), the distance from the spacecraft to the reconnection site is X_r=1±0.5 R_E. Qualitatively, this estimate places the spacecraft very close to the reconnection site that is located equatorward of the cusp.

In the cusp event in Figure 2, the nearly isotropic distribution observed in the magnetospheric-like magnetic field intervals was interpreted as the result of the evolution of the magnetic field line and the plasma as the magnetic field line convected sunward from the reconnection site. With a similar interpretation of the nearly isotropic distribution observed on lobe-like magnetic field lines in Figure 4, it is concluded that the field line convection was poleward away from the reconnection site for the cusp event on 11 April 1997 from 1430 to 1450 UT. The reconnection site and convection of the field line is illustrated in the schematic at the top

of Figure 3 although this type of reconnection is inherently 3-dimensional and the motion in the dawn/dusk direction is important [e.g., Fuselier et al., 1997]. The convection direction and reconnection site for this strongly northward IMF case are similar to what is typically observed for southward IMF [e.g., Onsager et al., 1993].

All distributions observed during the dayside magnetospheric-like magnetic field intervals between 1430 and 1450 UT had parallel propagating populations similar to the one in the right-hand side of Figure 4. Thus, reconnection equatorward of the cusp for this strongly northward IMF case was stable over at least this 20 minute time period.

4. Survey of high solar wind dynamic pressure cusp events

The key to locating a reconnection site poleward or equatorward of the cusp is the type of distribution observed during cusp intervals when the magnetic field had a dayside magnetospheric-like orientation. Comparing these distributions with those observed when the magnetic field had a lobe-like orientation helps identify the convection direction of the reconnected magnetic field. Nearly isotropic distributions during magnetospheric-like magnetic field intervals and "D" shaped distributions during lobe-like magnetic field intervals (Figure 2) are consistent with reconnection poleward of the cusp and sunward convection of the reconnected magnetic field lines. "D" shaped distributions during magnetospheric-like magnetic field intervals and nearly isotropic distributions during lobe-like magnetic field intervals (Figure 4) are consistent with reconnection equatorward of the cusp and poleward/tailward convection of the reconnected magnetic field lines. The observation of counterstreaming populations such as those in Figure 2 and 4 is not a necessary condition for determining the relative location of the reconnection site poleward or equatorward of the cusp [see also *Chandler et al.,* 1999]. The second population antiparallel to the magnetic field does permit a quantitative estimate of the distance to the reconnection site and confirms the location of the low altitude mirror point in the northern ionosphere. However, if the field line convection is

fast enough and the spacecraft is too close to the reconnection site, then the population that mirrors at low altitudes may not have sufficient time to return to the spacecraft.

Dayside magnetospheric-like magnetic field intervals are essential for determining the location of the reconnection site in the Polar data. These orientations occur only when the spacecraft is in the cusp under high solar wind dynamic pressure conditions. Thus, a survey of the occurrence of equatorward and poleward of the cusp reconnection using the Polar spacecraft data first requires the identification of these high solar wind dynamic pressure intervals. Using the Wind Solar Wind Experiment data, intervals between March 1996 (shortly after the Polar launch) and December 1998 (the end of the most recent cusp interval for Polar) when the solar wind density was ~3-4 times higher than an average of ~3 to 5 cm^{-3} and/or when the solar wind bulk flow velocity was ~200 km/s higher than an average of ~400 km/s were identified. Polar spacecraft intervals in the cusp under these high solar wind dynamic pressure conditions were confirmed by magnetosheath-like fluxes of protons measured by the TIMAS instrument. The magnetic field data from the Wind spacecraft was then checked and only those cusp intervals when the IMF was northward were used. Specifically, transitions to southward IMF were not included nor were northward IMF intervals that were within 5 to 10 minutes of transitions to southward IMF. This precaution was taken to account for possible errors in the estimated propagation time of the plasma and magnetic field between the Wind and Polar spacecraft and to allow some "settling" of the magnetospheric conditions after a change in the IMF clock angle. Finally, during these high solar wind dynamic pressure, northward IMF cusp intervals, the Polar magnetic field orientation was used to identify intervals when the magnetic field changed orientation from lobe-like to dayside magnetospheric-like.

Through this selection process, 17 cusp intervals were identified where the magnetic field had a dayside magnetospheric-like orientation for at least part of the cusp interval. Table 1 contains the dates and times of the 17 events and, for each event, the total number of minutes when the magnetic field had a magnetospheric-like orientation. These time intervals range from a low of about 1 minute during the 24 April 1998 event to a high of 151 minutes during the 29 May 1996

event. Also listed in the table are the most common type of ion distribution observed during the intervals when the magnetic field had a dayside magnetospheric-like orientation and the corresponding reconnection topology consistent with the most common type of ion distribution.

Of the 17 events, 9 had nearly isotropic distributions during most of the interval when the magnetic field had a dayside magnetospheric-like orientation. These 9 events consistent with reconnection poleward of the cusp include the 20 June 1996 interval discussed in Section 2 (see Figure 2). Five of the events had mostly "D" shaped distributions when the magnetic field had a magnetospheric-like orientation. These 5 events consistent with reconnection equatorward of the cusp include the 11 April 1997 interval discussed in Section 3 (see Figure 4) and the 29 May 1996 event discussed in detail by Chandler et al. [1999]. Finally, 3 events showed a mixture of the two types of distributions and are consistent with a mixture of the two reconnection topologies.

The magnetic field data from one of these mixed intervals is shown in Figure 5. The format is the same as for the magnetic field data in Figures 1 and 3. As with the other intervals, the model and observed magnetic field agree well for part of the interval (specifically, before 2140 and after 2240 UT) but deviate significantly from 2140 to 2240 UT when the observed B_z changes from negative to positive (i.e., from a lobe-like orientation to a dayside magnetospheric-like orientation).

Two distributions observed during the magnetospheric-like orientation are shown in Figure 6. The format is the same as in Figures 2 and 4 except that both distributions in Figure 6 were observed when the magnetic field orientation was magnetospheric-like. Despite the similar magnetic field orientation, the two distributions differ significantly. The distribution on the left-hand side resembles the "D" distributions in Figure 2 without the second proton population propagating antiparallel to the magnetic field. The distribution on the right-hand side resembles the nearly isotropic distributions in Figures 2 and 4. Figure 6 illustrates the finding that distributions consistent with antiparallel reconnection poleward of the cusp and component reconnection equatorward of the cusp can be observed in the course of the same cusp crossing. Other evidence that these reconnection topologies are mixed during a given cusp crossing are the cusp distributions

observed outside of the interval discussed in detail in Section 3 for the event on 11 April 1997 from 1430 to 1450 UT. D distributions are observed on lobe-like field lines outside of this interval (not shown). These distributions are consistent with reconnection poleward of the cusp. Thus, reconnection may not occur exclusively equatorward or poleward of the cusp for a given event.

Recognizing that either type of reconnection can occur in a given event, it is interesting to consider the total number of minutes a given reconnection topology is observed independent of the number of different events in the survey. For the 17 events in Table 1, the Polar spacecraft observed dayside magnetospheric-like magnetic fields for a total of 656 minutes. Of these 656 minutes, the TIMAS instrument observed proton distributions consistent with reconnection poleward of the cusp for a total of 308 minutes and proton distributions consistent with reconnection equatorward of the cusp for a total of 348 minutes. Thus, when considered on a total time basis, the two reconnection topologies are observed with approximately equal probability. It is important to note that almost one fourth of the total minutes of observations consistent with reconnection equatorward of the cusp come from a single event on 29 May 1996 [see also, *Chandler et al.,* 1999]. However, nearly one fifth of the total minutes of observations consistent with reconnection poleward of the cusp come from a single event on 26 June 1998.

Most interesting from a theoretical standpoint are the solar wind conditions which result in component reconnection equatorward of the cusp. Proton distributions consistent with either type of reconnection can be observed in a single cusp. However, errors in the propagation time between the Wind and Polar spacecraft will not allow the determination of the exact solar wind conditions to better than a few minutes accuracy. Thus, distinguishing changes in the solar wind conditions that lead to changes in the type of reconnection observed over the course of a cusp event is hampered by the uncertainty in determining the propagation of the solar wind conditions from the distant upstream site to the cusp event.

Returning to the original classification of the events in Table 1, Figure 7 shows the occurrence frequency as a function of the solar wind dynamic pressure. This figure illustrates the important selection criterion that all events had higher than nominal solar wind dynamic pressure.

Four of the five events with mostly reconnection equatorward of the cusp were among the seven events with the highest dynamic pressure.

Figure 8 shows the average solar wind B_{zGSM} versus the average solar wind B_{yGSM} for the 17 events. Error bars in Figure 8 are the standard deviation of the magnetic field measurements during the events. Four of the five events with reconnection mostly equatorward of the cusp had the largest values of solar wind B_z.

Finally, Figure 9 shows the average solar wind B_{zGSM} versus the average solar wind B_{xGSM} for the 17 events. All five events with reconnection mostly equatorward of the cusp had either the largest values of solar wind B_z, the largest values of solar wind B_x, or both. Two of the three events that were consistent with a mixture of both poleward and equatorward of the cusp reconnection also had high values of solar wind B_z, or B_x, or both.

5. Discussion and conclusions

In this paper, high solar wind dynamic pressure, northward IMF cusp events that had proton distributions consistent with antiparallel reconnection poleward of the cusp and component reconnection equatorward of the cusp were presented in Sections 2 and 3. The key to locating the reconnection site is the type of distribution observed during cusp intervals when the magnetic field had a dayside magnetospheric-like orientation. These intervals occur for the Polar spacecraft only when the solar wind dynamic pressure is high (see Figure 7). Under these conditions, the compression of the magnetopause moves the effective location of the spacecraft equatorward of the cusp and relatively near the magnetopause. Indeed, for the events in Sections 2 and 3, estimates indicate that the spacecraft was between 1 and 5 R_E from one magnetopause reconnection site and less than 1 R_E from another site.

The reconnection site does not necessarily remain either poleward or equatorward of the cusp during the course of a given event. Table 1 contains several events where a mixture of the

two reconnection topologies were observed (see Table 1). Even for events that had mostly one or the other topology, there were times during these events when the topology switched during the event. There are two interpretations for this mixture of topologies. Either the reconnection site switches so that at any given time it is occurring exclusively poleward or equatorward of the cusp or, more likely, different flux tubes have different magnetic topologies at the same time. A variation of the latter interpretation has been suggested previously. Nishida [1989] suggested a reconnection model for northward IMF where the magnetopause reconnection occurred over limited regions in a sporadic fashion on the dayside magnetopause. This model was introduced to explain the LLBL on dayside magnetic field lines for northward IMF and the small bulk flow observed in the layer. The model did not include reconnection poleward of the cusp, which is apparently important even when reconnection occurs equatorward of the cusp.

This type of sporadic reconnection is limited in space and unsteady in time. It may be an important element of reconnection equatorward of the cusp as the convection of the reconnected field lines is difficult to account for without both time and spatial variations [*Fuselier et al.,* 1997]. Nonetheless, on a given flux tube, reconnection equatorward of the cusp must be stable over many minutes and the magnetic field line convection must be very slow. For the cusp event in Section 3, proton distributions consistent with reconnection equatorward of the cusp were observed essentially uninterrupted for nearly 20 minutes (200 distributions at 6 second resolution). For the event on 29 May 1996 (Table 1) distributions consistent with reconnection equatorward of the cusp were observed nearly uninterrupted for over one and a half hours [see also *Chandler et al.,* 1999]. Furthermore, 10 minutes is required for a proton distribution to propagate along a reconnected flux tube to the ionosphere, mirror, and return to the Polar spacecraft at high latitudes. Thus, the distribution in the right-hand side of Figure 4 requires a stable flux tube topology, a well defined low altitude mirror point, and very slow convection over a period of at least 10 minutes. Other observations at the dayside subsolar magnetopause support these conclusions [*Onsager and Fuselier*, 1994; *Fuselier et al*., 1997].

Another difficult problem in the interpretation of these data presented here is the switching between magnetospheric-like and lobe-like magnetic field topologies. It is difficult to see how the effective location of the spacecraft can jump across the cusp rapidly as illustrated in Figures 1 and 3. Perhaps a different type of field line with both a magnetospheric-like and lobe-like orientation located entirely within the magnetopause is necessary to account for the abrupt magnetic field transitions in Figures 1 and 3. Such field lines are seen in MHD simulations [e.g., Wu, 1983, Figure 10]. However, these field lines must be contained entirely in the magnetosphere and they must not contain any pre-existing magnetosheath plasma prior to their reconnection.

At a given time, the probability of observing distributions consistent with reconnection equatorward of the cusp is nearly equal to the probability of observing distributions consistent with reconnection poleward of the cusp. To be sure, many events have a dominant reconnection topology. However, the longer intervals of equatorward of the cusp reconnection balance the more numerous events poleward of the cusp reconnection so that neither topology dominates. Whether one or the other topology dominates when the solar wind dynamic pressure is not high is an important question that cannot be answered with the present survey.

Of particular theoretical interest are the external conditions under which reconnection is initiated on field lines of a particular orientation. Previously, it was concluded that reconnection only occurs poleward of the cusp for northward IMF [e.g., *Crooker,* 1979]. Evidence suggests that this is not the case [*Sandholt et al.*, 1998], especially for high solar wind dynamic pressure conditions [*Onsager and Fuselier, 1994; Fuselier et al.,* 1997; *Chandler et al.,* 1999]. This study adds to this previous evidence and indicates that component reconnection equatorward of the cusp is at least as important as antiparallel reconnection when the solar wind dynamic pressure is high.

One way that component reconnection equatorward of the cusp may be facilitated for northward IMF is if the IMF has a large B_y (i.e., for large clock angle). Indeed, auroral emissions consistent with reconnection equatorward of the cusp were observed for northward IMF for clock angles greater than 45˚ [*Sandholt et al.*, 1998]. Surprisingly, most of the events consistent with reconnection equatorward of the cusp that are presented here have the smallest IMF clock angles.

Figure 8 shows that four of the five events consistent with reconnection equatorward of the cusp had the largest solar wind B_Z. These four events have IMF clock angles less than 30˚ and the events consistent with reconnection poleward of the cusp have larger IMF clock angles. This is the opposite correlation obtained from ground based observations discussed above. At present, there is no explanation for this discrepancy. However, the ground based observations and the observations in this paper were obtained under different conditions. In particular, the observations in this paper were made under high solar wind dynamic pressure while the ground based observations had no such restriction [M. Øieroset, personal communication, 1999].

All five events consistent with reconnection equatorward of the cusp and two of the three mixed events had either the largest solar wind B_Z or the largest solar wind B_X or both [Figure 9]. Large values of solar wind B_Z (small IMF clock angles) indicate that draped, dayside magnetosheath field lines equatorward of the cusp have very small angles relative to the magnetospheric field lines interior to the magnetopause. Furthermore, the IMF tends to rotate away from the shock normal across the Earth's bow shock, causing B_X to decrease and B_Z (or B_Y, in the case of large IMF clock angles) to increase in the subsolar magnetosheath. Thus, large IMF B_X and/or large B_Z is consistent with small angles between the dayside magnetospheric field and the magnetosheath magnetic field draped against the magnetopause.

While this result would appear to be contrary to expectations of reconnection [e.g., *Sonnerup,* 1974], high solar wind dynamic pressure may be a mitigating factor. High dynamic pressure and strongly northward IMF conditions produce strong plasma depletion at the dayside magnetopause. As the dynamic pressure and plasma depletion increases, the magnetosheath magnetic field increases, often to the point where the magnetosheath magnetic field is equal to or even greater than the magnetospheric field. Under these conditions, there is a component of the magnetosheath and magnetospheric fields that remains antiparallel down to near zero shear angle between the two fields [see *Anderson et al.*, 1997]. Indeed, distributions at the dayside magnetopause consistent with reconnection equatorward of the cusp were observed under high

solar wind dynamic pressure conditions for shear angles less than 30˚ between the magnetosheath and magnetospheric magnetic fields [*Fuselier et al.,* 1997].

In conclusion, this paper shows that reconnection equatorward of the cusp for high solar wind dynamic pressure, northward IMF conditions is as important as reconnection poleward of the cusp. The reconnection equatorward of the cusp may be sporadic but the topology of a given flux tube remains stable for many minutes. Favorable conditions for reconnection equatorward of the cusp are large IMF B_Z and/or B_X, which creates small shear angles between the draped magnetosheath field and the magnetospheric field. An important factor in this study may be the focus on high solar wind dynamic conditions. High solar wind dynamic pressure and northward IMF produce strong plasma depletion on the dayside magnetopause which may promote component reconnection down to very small clock angles [*Anderson et al.,* 1997]. Under more nominal solar wind dynamic conditions, larger clock angles may be necessary for reconnection equatorward of the cusp [e.g., *Sandholt et al.,* 1998].

Acknowledgments: The authors wish to thank K. Ogilvie and R. Lepping for providing solar wind context data through the NASA CDAWeb. The quality of these data and the ease at which they were obtained greatly facilitated this study. Also, discussions with M. Lockwood were very beneficial. The TIMAS investigation is the result of many years of work by a large group of dedicated scientists and engineers. The development of the mass spectrometer was lead by E. G. Shelley (retired principal investigator). Research at Lockheed Martin was conducted under the TIMAS data analysis contract with NASA, NAS5-30302. Research at the University of California, Los Angeles was conducted under contract with NASA

References

Anderson, B. J., T. D. Phan, and S. A. Fuselier, Relationships between plasma depletion and subsolar reconnection, *J. Geophys. Res., 102*, 9531, 1997.

Chandler, M. O., S. A. Fuselier, M. Lockwood, and T. E. Moore, Observations of ion signatures of low shear magnetic merging, *Geophys. Res. Lett.*, in press, 1999.

Cowley, S. W. H., The causes of convection in the Earth's magnetosphere: A review of developments during the IMS, *Rev. Geophys. 20*, 531, 1982.

Crooker, N. Dayside merging and cusp geometry, *J. Geophys. Res., 84*, 951, 1979.

Dungey, J. W., Interplanetary magnetic field and the auroral zones, *Phys. Rev. Lett., 6*, 47, 1961.

Dungey, J. W., The structure of the ionosphere, or adventures in velocity space, in *Geophysics: The Earth's Environment*, edited by C. DeWitt, J. Hiebolt, and A. Lebeau, p. 526-536, Gordon and Breach, New York, 1963.

Fuselier, S. A., B. J. Anderson, and T. G. Onsager, Particle signatures of magnetic topology at the magnetopause: AMPTE/CCE observations, *J. Geophys. Res., 100*, 11,805, 1995.

Fuselier, S. A., B. J. Anderson, and T. G. Onsager, Electron and ion signatures of field line topology at the low-shear magnetopause, *J. Geophys. Res., 102*, 4847, 1997.

Gosling, J. T., M. F. Thomsen, S. J. Bame, R. C. Elphic, and C. T. Russell, Plasma flow reversals at the dayside magnetopause and the origin of asymmetric polar cap convection, *J. Geophys. Res., 95*, 8073, 1990.

Gosling, J. T., M. F. Thomsen, S. J. Bame, R. C. Elphic, and C. T. Russell, Observations of reconnection of interplanetary and lobe magnetic field lines at the high-latitude magnetopause, *J. Geophys. Res., 96*, 14,097, 1991.

Kessel, R. L., S.-H. Chen, J. L. Green, S. F. Fung, S. A. Boardsen, L. C. Tan, T. E. Eastman, J. D. Craven, and L. A. Frank, Evidence of high-latitude reconnection during northward IMF: Hawkeye observations, *Geophys. Res. Lett., 23*, 583, 1996.

Lepping, R. P., et al., The wind magnetic field investigation, in *The Global Geospace Mission*, ed. by C. T. Russell, p. 207, Kluwer Academic Publishers, Dordrecht, 1995.

Maezawa, K. Magnetospheric convection induced by the positive and negative z components of the interplanetary magnetic field: Quantitative analysis using polar cap magnetic records, *J. Geophys. Res., 81*, 2289, 1976.

Nishida, A., Can random reconnection on the magnetopause produce the low latitude boundary layer, *Geophys. Res. Lett., 16*, 227, 1989.

Ogilvie, K. W., et al., A comprehensive plasma instrument for the Wind spacecraft, in *The Global Geospace Mission*, ed. by C. T. Russell, p. 55, Kluwer Academic Publishers, Dordrecht, 1995.

Øieroset, M., P. E. Sandholt, W. F. Denig, and S. W. H. Cowley, Northward interplanetary magnetic field cusp aurora and high-latitude magnetopause reconnection, *J. Geophys. Res., 102*, 11,349, 1997.

Onsager, T. G., M. F. Thomsen, J. T. Gosling, and S. J. Bame, Electron distributions in the plasma sheet boundary layer: Time-of-flight effects, *Geophys. Res. Lett., 17*, 1837, 1990.

Onsager, T. G., C. A. Kletzing, J. B. Austin, and H. MacKiernan, Model of magnetosheath plasma in the magnetosphere: Cusp and mantle particles at low altitudes, *Geophys. Res. Lett., 20*, 479, 1993.

Onsager, T. G., and S. A. Fuselier, The location of magnetic reconnection for northward and southward interplanetary magnetic field, in *Solar System Plasmas in Space and Time, Geophys. Monogr. Ser. vol. 84*, edited by J. L. Burch and J. H. Waite, Jr., p. 183, AGU, Washington, D. C., 1994.

Onsager, T. G., S.-W. Chang, J. D. Perez, J. B. Austin, and L. X. Janou, Low-altitude observations and modeling of quasi-steady magnetopause reconnection, *J. Geophys. Res., 100*, 11,831, 1995.

Petrinec, S. M., and C. T. Russell, Near-Earth magnetotail shape and size as determined from the magnetopause flaring angle, *J. Geophys. Res., 101*, 137, 1996.

Russell, C. T., The configuration of the magnetosphere, in *Critical Problems of Magnetospheric Physics*, edited by E. R. Dyer, p. 1, Inter-Union Commission on Solar-Terrestrial Physics, Secretariat, National Academy of Sciences, Washington, D. C., 1972.

Russell, C. T., R. C. Snare, J. D. Means, D. Pierce, D. Dearborn, M. Larson, G. Barr, and G. Le, The GGS/Polar magnetic fields investigation, in *The Global Geospace Mission*, ed. by C. T. Russell, p. 563, Kluwer Academic Publishers, Dordrecht, 1995.

Sandholt, P. E., C. J. Farrugia, J. Moen, Ø. Noraberg, B. Lybekk, T. Sten, and T. L. Hansen, A classification of dayside auroral forms and activities as a function of IMF orientation, *J. Geophys. Res.*, in press, 1998.

Shelley, E. G., et al., The toroidal imaging mass-angle spectrograph (TIMAS) for the Polar mission, in *The Global Geospace Mission*, ed. by C. T. Russell, p. 497, Kluwer Academic Publishers, Dordrecht, 1995.

Sonnerup, B. U. O., Magnetopause reconnection rate, *J. Geophys. Res.*, *79*, 1546, 1974.

Woch J., and R. Lundin, Magnetosheath plasma precipitation in the polar cusp and its control by the interplanetary magnetic field, *J. Geophys. Res.*, *97*, 1421, 1992.

Wu, C. C., Shape of the magnetosphere, *Geophys. Res. Lett.*, *10*, 545, 1983.

Table 1. Events with magnetospheric magnetic field orientation

Date	Time	Total Minutes with Magnetospheric Magnetic Field Orientation	Most common ion distribution observed	Most common reconnection site location relative to the cusp
29-May-96*	0409-0700	151	D-shaped	equatorward
20-Jun-96	0454-0558	14	isotropic	poleward
23-Aug-96	0045-0154	65	isotropic	poleward
11-Apr-97	1434-1451	15	D-shaped	equatorward
15-May-97	0822-0838	9	isotropic	poleward
22-May-97	0315-0412	8	isotropic	poleward
4-Aug-97	0123-0159	6	Mixture	Mixture
4-Apr-98	1657-1712	11	isotropic	poleward
24-Apr-98	0310-0311	1	isotropic	poleward
30-Apr-98	1754-1815	6	Mixture	Mixture
2-May-98	0519-0602	37	D-shaped	equatorward
6-Jun-98	0549-0626	13	isotropic	poleward
18-Jun-98	2140-2205	25	isotropic	poleward
25-Jun-98	1120-1410	95	D-shaped	equatorward
26-Jun-98	0808-0939	89	isotropic	poleward
31-Jul-98	2140-2236	45	Mixture	Mixture
26-Aug-98	0722-0912	66	D-shaped	equatorward

* see also Chandler et al., 1999

Figure Captions

Figure 1. (Top) Noon-midnight meridian cut through the magnetosphere showing the Polar spacecraft location for 20 June 1996 from 0300 to 0800 UT. (Bottom) The three GSM components and the magnitude of the magnetic field measured in the cusp from 0300 to 0800 UT. The observed (solid lines) and model (dashed lines) magnetic field agree reasonably well before 0450 UT and after 0700 UT. Between 0450 and 0700 UT, the measured magnetic field often has a dayside magnetospheric orientation ($B_x<0$, $B_z>0$) when the model magnetic field predicts a lobe-like orientation ($B_x>0$, $B_z<0$).

Figure 2. Two dimensional cuts in the velocity space distribution in a plane containing the magnetic field (y axis) and the Earth-sun line (top panels) and one dimensional cuts along the magnetic field (bottom panels). These distributions are from the cusp interval in Figure 1 when the magnetic field had a lobe-like orientation (left-hand side), and when it had a dayside magnetospheric-like orientation (right-hand side). When the magnetic field had a lobe-like orientation, the proton distribution consisted of two distinct populations. The lower energy, higher flux, parallel propagating population came directly from the high latitude reconnection site poleward of the cusp. The higher energy, lower flux, antiparallel propagating distribution propagated along the magnetic field from the reconnection site, mirrored at low altitudes in the northern ionosphere, and returned to the spacecraft. The distribution on the right-hand side resembles a nearly isotropic distribution with a small bulk flow parallel to the magnetic field.

Figure 3. (Top) Noon-midnight meridian cut through the magnetosphere showing the Polar spacecraft location for 11 April 1997 from 1100 to 1600 UT. (Bottom) The three GSM

components and the magnitude of the magnetic field measured in the cusp from 1100 to 1600 UT. The format is the same as in Figure 1. The observed (solid lines) and model (dashed lines) magnetic field agree reasonably well except for the interval from 1430 to 1450 UT. In this interval, the observed magnetic field has a dayside magnetospheric-like orientation.

Figure 4. Two dimensional cuts in the velocity space distribution in a plane containing the magnetic field (y axis) and the Earth-sun line (top panels) and one dimensional cuts along the magnetic field (bottom panels). The format is the same as in Figure 2. When the magnetic field had a dayside magnetospheric-like orientation, the proton distribution (right-hand side) consisted of two distinct populations. The lower energy, higher flux, parallel propagating population came directly from the low latitude reconnection site equatorward of the cusp. The higher energy, lower flux, antiparallel propagating distribution propagated along the magnetic field from the reconnection site, mirrored at low altitudes in the northern ionosphere, and returned to the spacecraft. The distribution on the left-hand side resembles a nearly isotropic distribution with a small bulk flow parallel to the magnetic field.

Figure 5. The three GSM components and the magnitude of the magnetic field measured in the cusp on 31 July 1998 from 2100 to 2300 UT. The observed (solid lines) and model (dashed lines) magnetic field agree reasonably well except for the interval from about 2130 to 2240 UT. In this interval, the observed magnetic field often has a dayside magnetospheric-like orientation.

Figure 6. Two dimensional cuts in the velocity space distribution in a plane containing the magnetic field (y axis) and the Earth-sun line (top panels) and one dimensional cuts along the magnetic field (bottom panels). The format is the same as in Figures 2 and 4 except that both distributions were observed when the magnetic field had a dayside magnetospheric-like orientation. The proton distribution on the left-hand side is a low-energy, high flux, parallel propagating distribution that came directly from the low latitude reconnection site equatorward of the cusp. The

distribution on the right-hand side was measured almost 20 minutes later and resembles a nearly isotropic distribution with a small bulk velocity parallel to the magnetic field.

Figure 7. Solar wind dynamic pressures for the 17 cusp events consistent with reconnection mostly poleward of the cusp, mostly equatorward of the cusp, and a mixture of both topologies. All events occurred for solar wind dynamic pressures between two and ten times higher than the typical solar wind dynamic pressure. Four of the five events consistent with reconnection equatorward of the cusp were among the seven events with the highest solar wind dynamic pressure.

Figure 8. Solar wind magnetic field B_z and B_y for the 17 cusp events consistent with reconnection mostly poleward of the cusp, mostly equatorward of the cusp, and a mixture of both topologies. Four of the five events consistent with reconnection mostly equatorward of the cusp had the largest B_z of all events. Furthermore, these four events had IMF clock angles less than 30˚.

Figure 9. Solar wind magnetic field B_z and B_x for the 17 cusp events consistent with reconnection mostly poleward of the cusp, mostly equatorward of the cusp, and a mixture of both topologies. The five events consistent with reconnection mostly equatorward of the cusp and two of three events that were a mixture of the two reconnection topologies had either the largest B_z, the largest B_x, or the largest of both components.

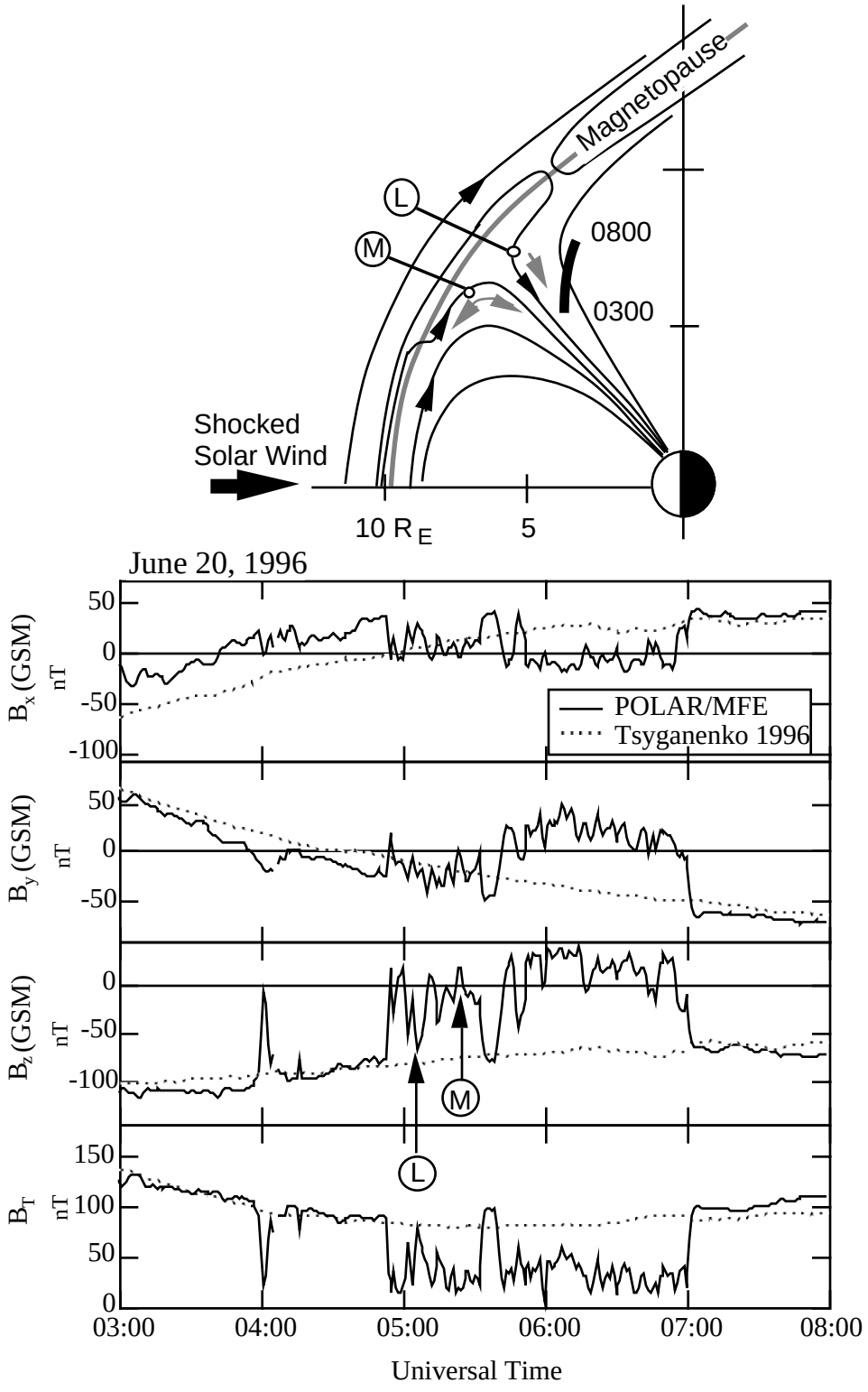
Magnetopause
L
M
0800
0300
Shocked
Solar Wind
10 R E
5
June 20, 1996
B x (GSM)
nT
50
0
-50
-100
POLAR/MFE
Tsyganenko 1996
B y (GSM)
B z (GSM)
B T
150
100
03:00
04:00
05:00
06:00
07:00
08:00
Universal Time

Figure 1

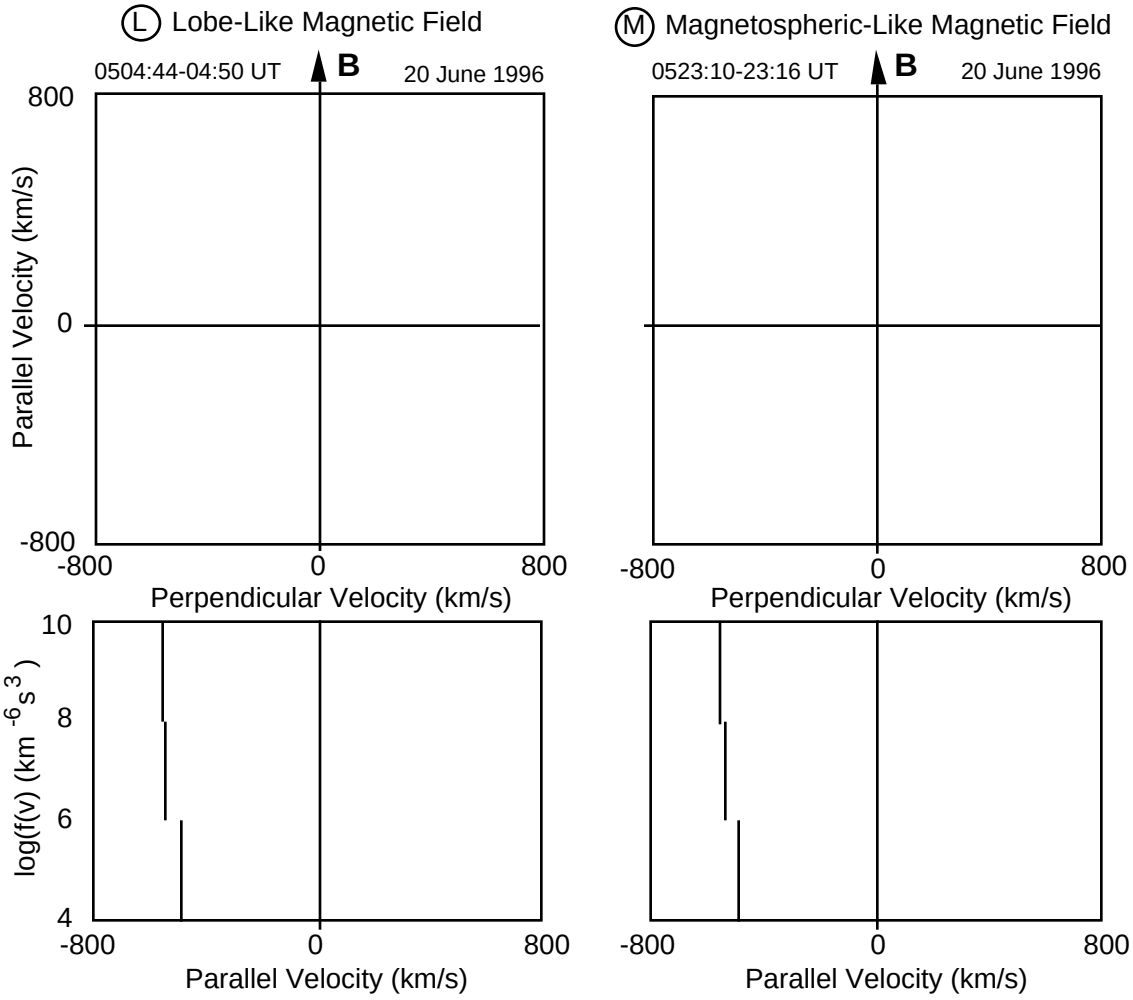

Figure 2 (placeholder)

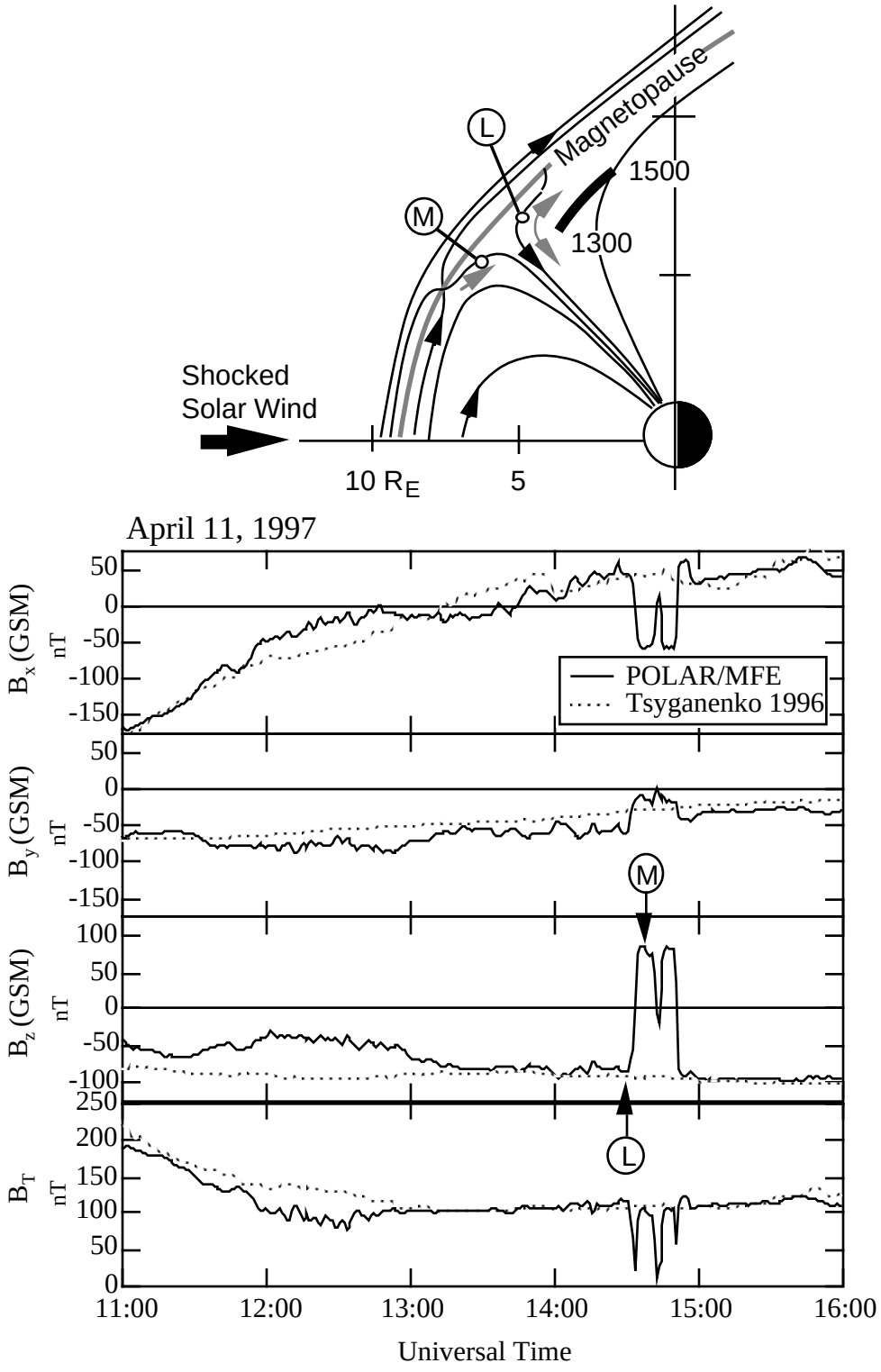
Magnetopause
L
M
1500
1300
Shocked
Solar Wind
10 R_E
5
April 11, 1997
B_x (GSM)
B_y (GSM)
B_z (GSM)
B_T
nT
POLAR/MFE
Tsyganenko 1996
M
L
11:00
12:00
13:00
14:00
15:00
16:00
Universal Time

Figure 3

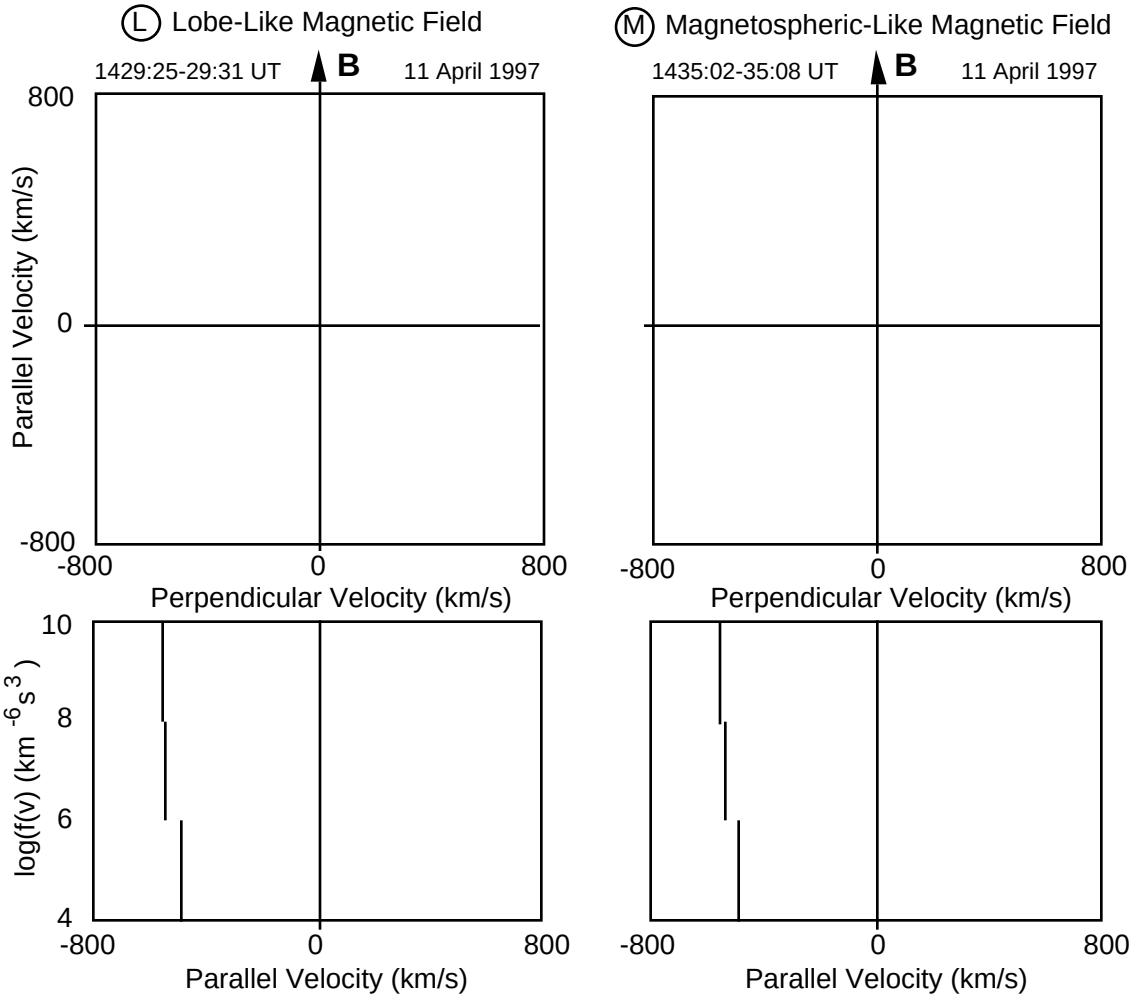

Figure 4 (placeholder)

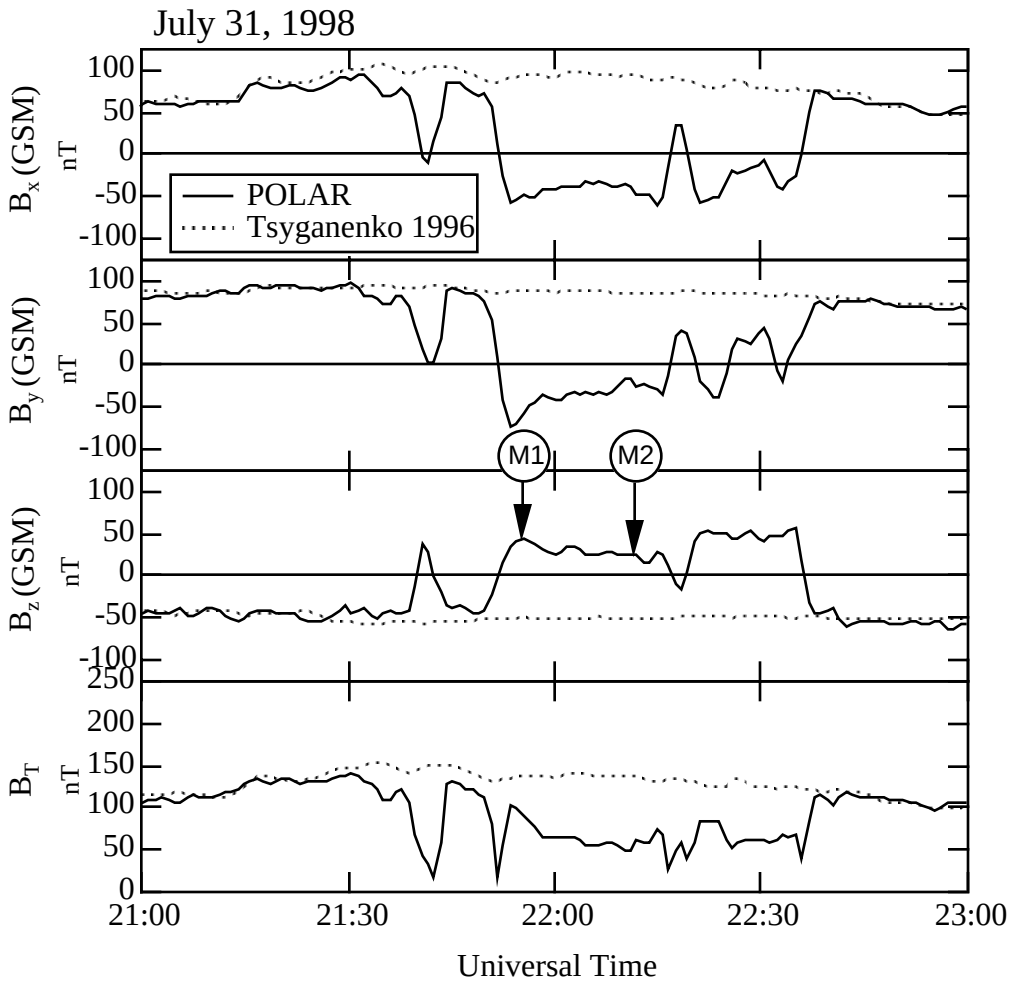
July 31, 1998
B_x (GSM)
nT
B_y (GSM)
nT
B_z (GSM)
nT
B_T
nT
POLAR
Tsyganenko 1996
M1
M2
100
50
0
-50
-100
250
200
150
21:00
21:30
22:00
22:30
23:00
Universal Time

Figure 5

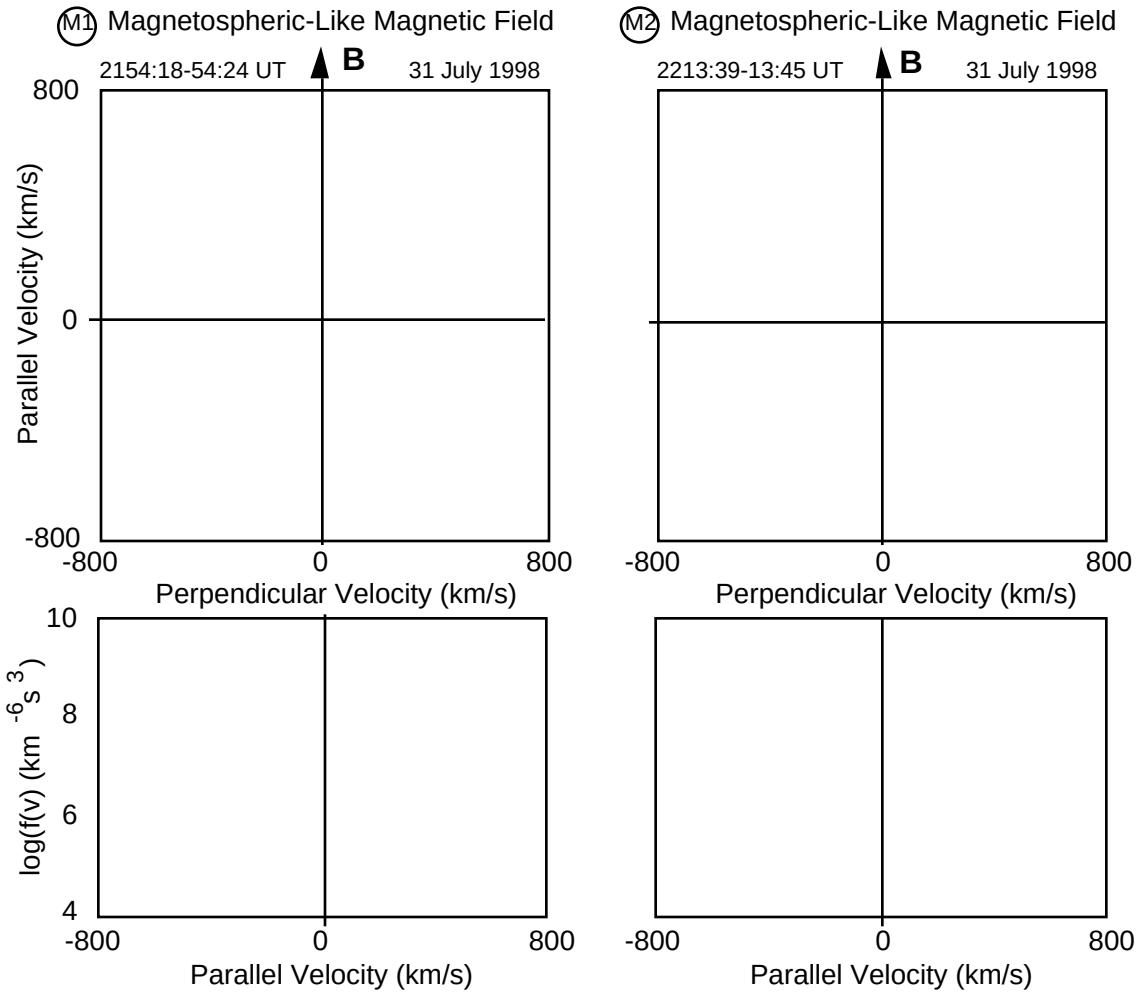

Figure 6 (placeholder)

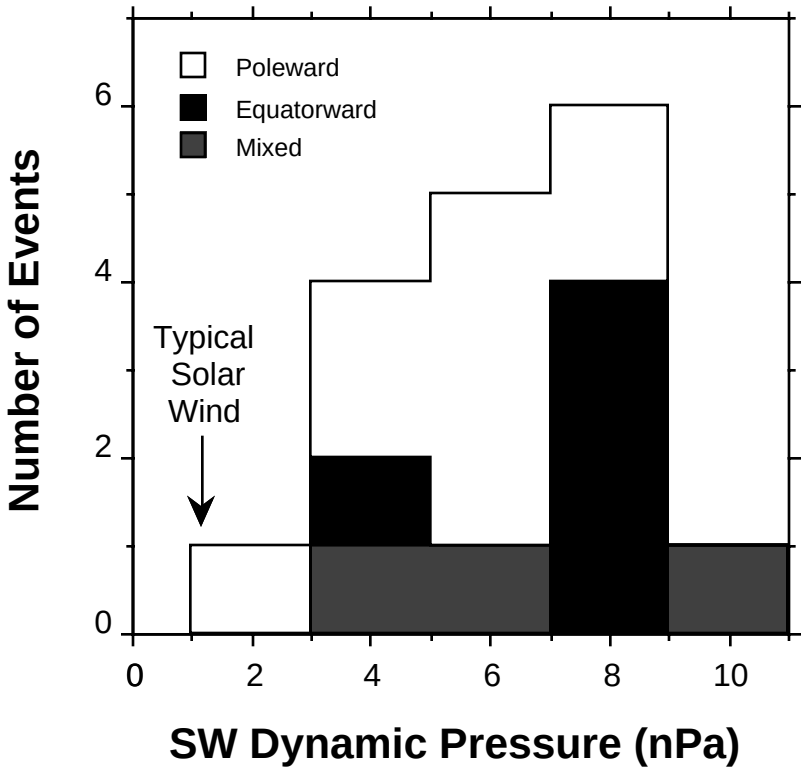
Poleward
Equatorward
Mixed
Typical
Solar
Wind
Number of Events
SW Dynamic Pressure (nPa)
0
2
4
6
8
10

Figure 7

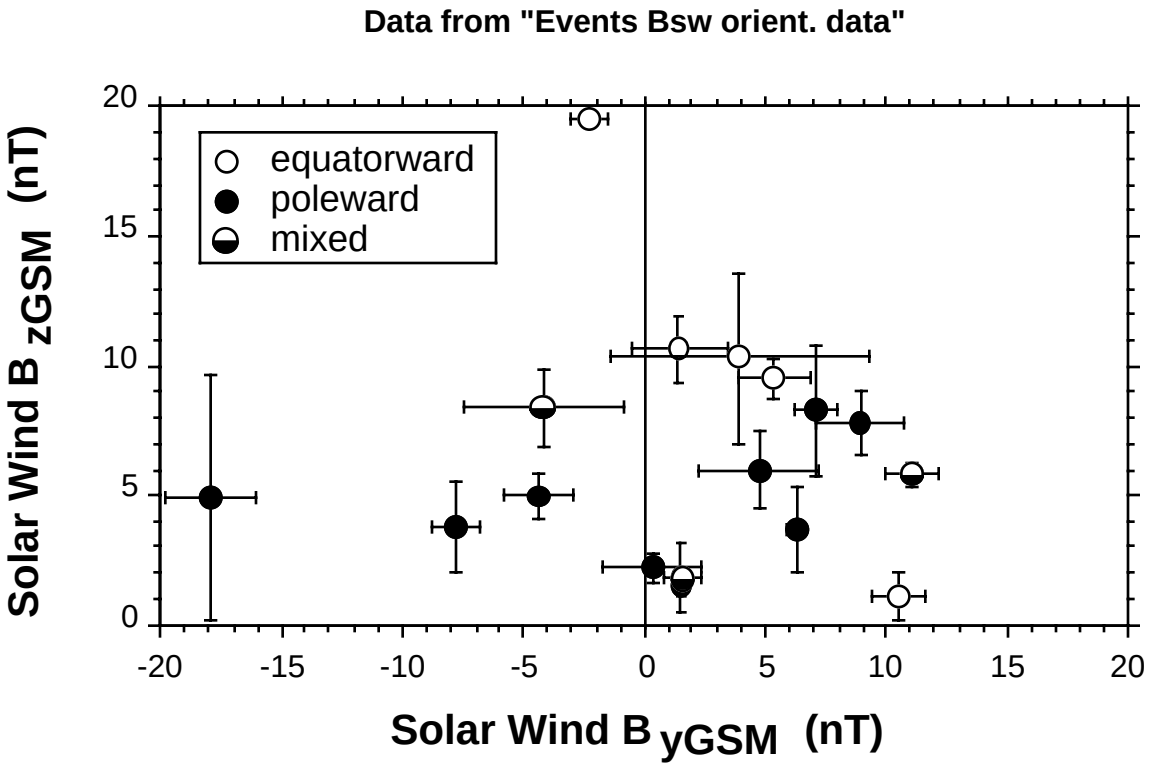
Data from "Events Bsw orient. data"
equatorward
poleward
mixed
Solar Wind B zGSM (nT)
Solar Wind B yGSM (nT)
20
15
10
5
0
-20
-15
-10
-5
0
5
10
15
20

Figure 8

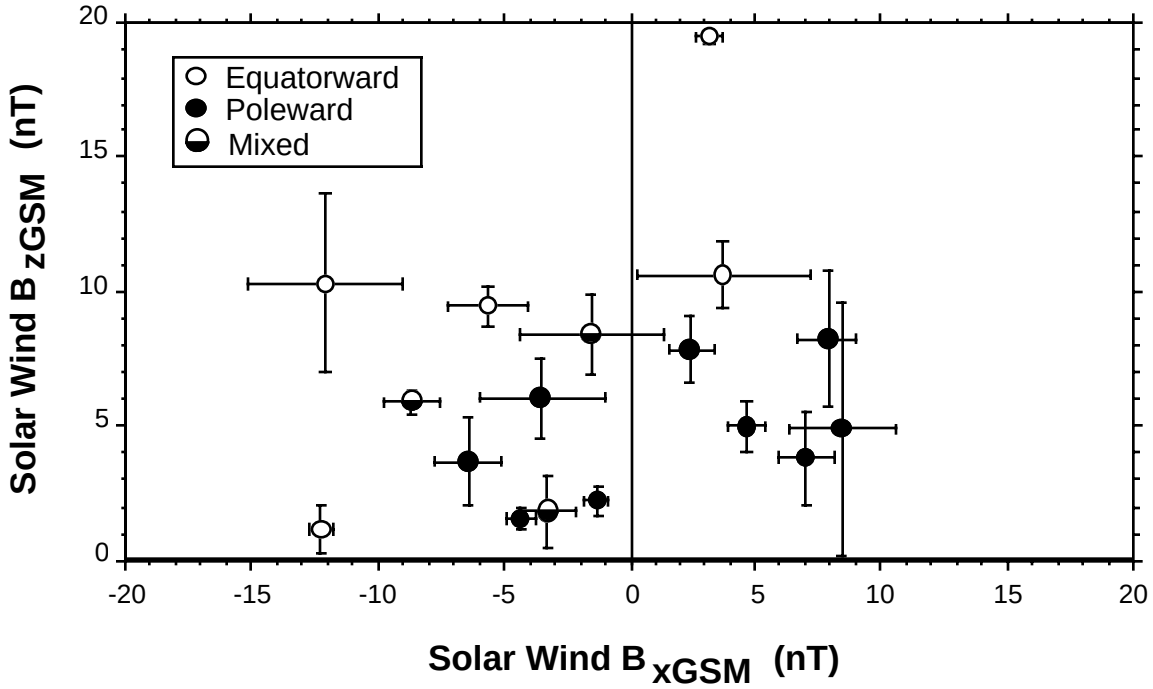
Equatorward
Poleward
Mixed
Solar Wind B zGSM (nT)
Solar Wind B xGSM (nT)
20
15
10
5
0
-20
-15
-10
-5
0
5
10
15
20

Figure 9